Scientific Research Publishing

Journal of Materials Science and Chemical Engineering, 2018, 6, 31-49
http://www.scirp.org/journal/msce
ISSN Online: 2327-6053
ISSN Print: 2327-6045

7-(2-Ethyltiophenyl) Theophylline as Copper Corrosion Inhibitor in 1M HNO_3

Ouédraogo Augustin[1], Akpa Sagne Jacques[2], Diki N'guessan Yao Silvère[1*], Diomande Gbe Gondo Didier[2], Coulibaly Nagnonta Hippolyte[1], Trokourey Albert[1]

[1]Laboratoire de Chimie Physique, Université Félix Houphouët-Boigny, Abidjan, Côte d'Ivoire
[2]Laboratoire de Chimie Organique et Substances Naturelles, Université Félix Houphouët-Boigny, Abidjan, Côte d'Ivoire
Email: *dickiensil2@gmail.com

How to cite this paper: Augustin, O., Jacques, A.S., N'guessan Yao Silvère, D., Didier, D.G.G., Hippolyte, C.N. and Albert, T. (2018) 7-(2-Ethyltiophenyl) Theophylline as Copper Corrosion Inhibitor in 1M HNO_3. *Journal of Materials Science and Chemical Engineering*, **6**, 31-49.
https://doi.org/10.4236/msce.2018.68004

Received: August 3, 2018
Accepted: August 28, 2018
Published: August 31, 2018

Abstract

7-(2-ethyltiophenyl) theophylline was used as copper corrosion inhibitor in 1M HNO_3 solution. The study was performed using mass loss, scanning electron microscopy (SEM) and Density Functional Theory (DFT) methods. The results show that the inhibition efficiency increases up to 91.29% with increase of the inhibitor concentration (from 0.05 to 5 mM) but decreases with raising temperature of the solution. Copper dissolution was found to be temperature and 7-(2-ethyltiophenyl) theophylline concentration dependent. The thermodynamic functions related to the adsorption of the molecule on the copper surface and that of the metal dissolution were determined. The results point out a spontaneous adsorption and an endothermic dissolution processes. Adsorption models including Langmuir, El-Awady and Flory-Huggins isotherms were examined. The results also suggest spontaneous and predominant physical adsorption of 7-(2-ethyltiophenyl) theophylline on the metal surface which obeys Langmuir isotherm model. Further investigation on the morphology using scanning electron microscopy (SEM) has confirmed the existence of a protective film of inhibitor molecules on copper surface. Furthermore, the global and local reactivity parameters of the studied molecule were analyzed. Experimental and theoretical results were found to be in good agreement.

Keywords

Corrosion, 7-(2-Ethyltiophenyl) Theophylline, Mass Loss, SEM, DFT

1. Introduction

Copper [1] [2] [3] [4] is widely applied in many industries and applications (in-

dustrial equipment, electricity and electronics, communications, pipelines for domestic and industrial water utilities, etc.) due to its excellent electrical and mechanical properties and low prices. Thus corrosion of copper and its inhibition in aggressive media, particularly in presence of chloride ions [5] [6] [7] [8], have attracted the attention of many research teams.

One of the most important methods in copper protection against corrosion is the use of organic inhibitors containing polar groups, including nitrogen, sulfur and oxygen [9] [10] [11]. Nowadays, heterocyclic compounds with polar functional groups and conjugated double bonds are frequently used for copper corrosion inhibition [12]. The inhibiting action of these organic compounds [13] [14] is usually attributed to their interactions with the copper surface via adsorption which depends on the nature of the copper/solution interface.

Recently, the effectiveness of an inhibitor molecule [15] [16] [17] has been related to its spatial as well as electronic structure. Quantum chemical methods are ideal tools for investigating these parameters and are able to provide insight into the inhibitor-surface interaction. A variety of chemical concepts which are now widely used as descriptors of chemical reactivity, e.g., electronegativity [18], hardness or softness [19], etc., appear within DFT. The Fukui function [20] and the local softness [21] measure the local electron density/population displacements corresponding to the inflow of single electron. They have been successfully performed [22] [23] to link the corrosion inhibition efficiency with molecular orbital (MO) energy levels for many organic compounds.

The aim of the present paper is to study the behavior of 7-(2-ethyltiophenyl) theophylline (**Scheme 1**) by analyzing its inhibition efficiency both on the experimental and theoretical points of views. Theoretical parameters such as the energy of the highest occupied molecular orbital (E_{HOMO}), the energy of lowest unoccupied molecular orbital (E_{LUMO}), the energy gap (ΔE) between E_{LUMO} and E_{HOMO}, the dipole moment (μ), the ionization energy (I), the electron affinity (A), the electronegativity (χ), the global hardness (η), the global softness (S), the electrophilicity index (ω), the fraction of electrons transferred (ΔN) are determined and analyzed. The local reactivity has been analyzed through the Fukui indices, since they indicate the reactive regions in the form of nucleophilic and electrophilic behavior of each atom in the molecule.

2. Experimental

2.1. Copper Specimen

The samples of copper used in this study were in the form of rods with 10 mm as

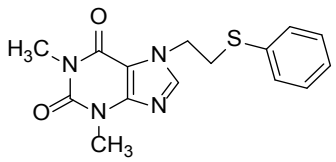

Scheme 1. Chemical structure of 7-(2-ethyltiophenyl) theophylline.

length and 2.2 mm as diameter which were cut in commercial copper of purity 95%.

2.2. Reagents

The structure of 7-(2-ethyltiophenyl) theophylline has $C_{15}H_{16}N_4O_2S$ as formula. It is a kaki color powder provided by the Laboratory of Organic Chemistry and Natural Substances, Felix Houphouet-Boigny University. Its molecular structure was identified by ^1H NMR and ^{13}C NMR spectroscopy:

-RMN ^1H (CDCl3, Δ ppm): 3.40 (s, 3H, CH_3^-); 3.49 (t, 2H, $N\text{-}CH_2^-$); 3.50 (s, 3H, CH_3^-); 4.43 (t, 2H, $-CH_2$-S); 7.25(m, 5H, H_{Ar}); 7.48 (s, 1H, $N=CH^-$).

-RMRN ^{13}C (CDCl3, Δ ppm): 29.73 (CH_3^-); 29.90 (CH_3^-); 34.65 ($N\text{-}CH_2^-$); 47.08 ($-CH_2$-S); 126.75 (C_{Ar}); 127.50 (C_{Ar}); 128.89 (C_{Ar}); 129.05 (C_{Ar}); 130.17 (C_{Ar}); 133.95 (C_{Ar}).

Commercial nitric acid of purity 65% was purchased from Pan Reac Appli-Chem.

2.3. Solution Preparation

1M HNO_3 solutions without or with different concentrations of 7-(2-ethyltiophenyl) theophylline ranging from 0.05 to 5 mM were then prepared.

2.4. Mass Loss Measurement

Before each measurement, the copper samples were mechanically abraded with different grade emery papers (1/0, 2/0, 3/0, 4/0, 5/0, and 6/0). The specimens were washed thoroughly with bidistilled water, degreased and rinsed with acetone and dried in an oven. Mass loss measurements were performed in a beaker of 100 mL capacity containing 50 mL of the test solution. The immersion time for mass loss was 1h at a given temperature. In order to get good reproducible data, parallel triplicate experiments were conducted accurately and the average mass loss was used to evaluate the corrosion rate (W), the degree of surface coverage (θ) and the inhibition efficiency (IE) using Equations (1)-(3) respectively:

$$W = \frac{m_1 - m_2}{St} \tag{1}$$

$$\theta = \frac{W_0 - W}{W_0} \tag{2}$$

$$IE(\%) = \left(\frac{W_0 - W}{W_0}\right) * 100 \tag{3}$$

where W_0 and W are the corrosion rate without and with inhibitor respectively, m_1 and m_2 are the mass before and after immersion in the corrosive aqueous solution respectively, S is the total surface of the copper specimen and t is the immersion time.

2.5. Scanning Electron Microscopy

The scanning electron microscopy (FEG SEM, SUPRA 40 VP, ZEISS, Germany)

was used to characterize the copper surface after its treatment in the presence or absence of 7-(2-ethyltiophenyl) theophylline for 1 h immersion in 1M HNO_3 at 303 K. Comparison was made between the bare sample and the immersed ones.

2.6. Quantum Chemistry

To calculate the ground-state energy and the physical properties of 7-(2-ethyltiophenyl) theophylline, the Gaussian 09 W package [24] was used. The molecular structure was optimized to a minimum without symmetry restrictions using B3LYP exchange correlation functional, a combination of the Becke three parameter hybrid functional [25] with the correlation functional of Lee, Yang and Parr [26] [27] associated to 6-31 G (d, p) basis set [28]. **Figure 1** presents the optimized structure of 7-(2-ethyltiophenyl) theophylline. Density functional theory has been proved to be successful in providing theoretical basis for chemical concepts such as electronegativity (χ), hardness (η), softness (S) and local parameters as Fukui function $\left(f(r)\right)$, and local softness $\left(s(r)\right)$.

For N-electrons system with total energy E, the electronegativity is given by Equation (4):

$$\chi = -\mu_P = -\left(\frac{\partial E}{\partial N}\right)_{v(r)} \tag{4}$$

where μ_P and $v(r)$ are the chemical and external potentials respectively. The chemical hardness η which is defined as the second derivative of E with respect to N is then given by Equation (5):

$$\eta = \left(\frac{\partial^2 E}{\partial N^2}\right)_{v(r)} \tag{5}$$

The global softness S is the inverse of the global hardness as seen in Equation (6):

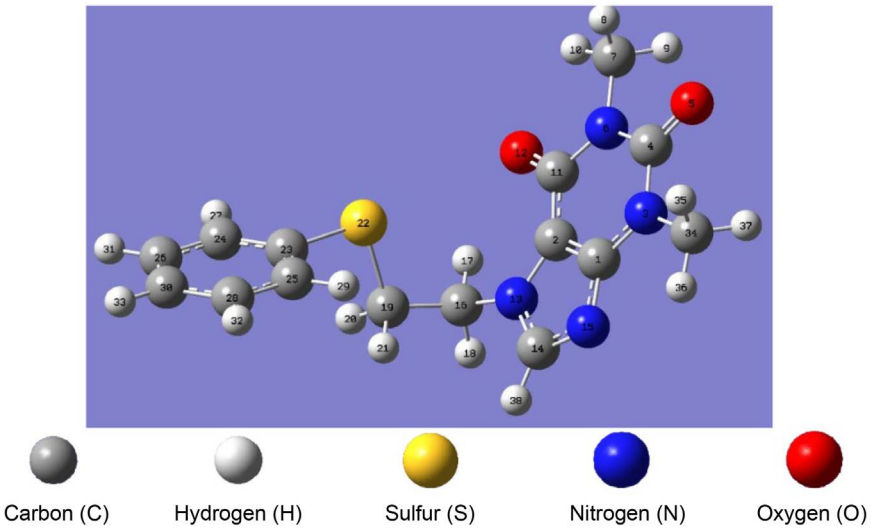

Figure 1. Optimized structure of 7-(2-ethyltiophenyl) theophylline by B3LYP/6-31G (d, p).

$$S = \frac{1}{\eta} \tag{6}$$

According to Koopman's theorem [29], the ionization potential I can be approximated as the negative of the highest occupied molecular orbital (HOMO) energy:

$$I = -E_{\text{HOMO}} \tag{7}$$

The negative of the lowest unoccupied molecular orbital (LUMO) energy is related to the electron affinity A:

$$A = -E_{\text{LUMO}} \tag{8}$$

The electronegativity was obtained using the ionization energy I and the electron affinity A as given in Equation (9):

$$\chi = \frac{I + A}{2} \tag{9}$$

The hardness which is the reciprocal of the electronegativity was obtained by Equation (10):

$$\eta = \frac{I - A}{2} \tag{10}$$

When the organic molecule is in contact with the metal, electrons flow from the system with lower electronegativity to that of higher electronegativity until the chemical potential becomes equal. The fraction of electrons transferred, ΔN, was estimated according to Pearson [30]:

$$\Delta N = \frac{\chi_{Cu} - \chi_{inh}}{2\left(\eta_{Cu} + \eta_{inh}\right)} \tag{11}$$

In this study, we used theoretical values of χ_{Cu} and η_{Cu} ($\chi_{Cu} = 4.98$ eV [31] and $\eta_{Cu} = 0$ [32]).

The global electrophilicity index, introduced by Parr [31] is given by Equation (12):

$$\omega = \frac{\chi^2}{2\eta} \tag{12}$$

The local selectivity of a corrosion inhibitor [33] is generally assessed using Fukui functions. Their values are used to identify which atoms in the inhibitor are more prone to undergo an electrophilic or nucleophilic attack. The change in electron density [34] is the nucleophilic and electrophilic Fukui functions, which are defined as:

$$f(r) = \left(\frac{\partial \rho(r)}{\partial N}\right)_{v(r)} \tag{13}$$

where N and $\rho(r)$ are the number of electrons and the electron density at position r of the chemical species respectively. After taking care of the discontinuities in $f(r)$ versus N plot, the "condensed-to-atom" approximations of $f(r)$, when multiplied by global softness (S) [35] provide local softness values

given by Equations (14)-(15) respectively:

$$s_k^+(r) = \left[q_k(N+1) - q_k(N)\right]S = f_k^+ S \quad (14)$$

$$s_k^-(r) = \left[q_k(N) - q_k(N-1)\right]S = f_k^- S \quad (15)$$

In these equations $q_k(N+1)$, $q_k(N)$ and $q_k(N-1)$ represent the condensed electronic populations on atom "*K*" for anionic, neutral and cationic systems respectively. Therefore, $s_k^+(r)$ and $s_k^-(r)$ represent the condensed local softness values of atom "*K*" towards nucleophilic and electrophilic attacks.

3. Results and Discussion

3.1. Effect of Concentration and Temperature

The corrosion rate curves of copper without and with the addition of 7-(2-ethyltiophenyl) theophylline in 1M HNO_3 at different temperatures are shown in Figure 2. These curves indicate that corrosion rate of copper in the studied medium, increases with increasing temperature of the solution. But this evolution is moderated when the concentration of the studied inhibitor increases, revealing the effectiveness of the molecule as a corrosion inhibitor for copper in 1M HNO_3. These results could be interpreted as the formation of a film barrier which isolates the metal from its aggressive environment.

For the temperature range studied, the inhibition efficiency (IE) increases with the increase in inhibitor concentration until a value of 91.29% for the concentration of 5 mM at 303 K (Figure 3).

As highlighted in Figure 3, the inhibition efficiency decreases with the rise in temperature for the concentration range studied. The evolution of the inhibition efficiency for each concentration of 7-(2-ethyltiophenyl) theophylline shows a significant decrease in corrosion rate upon the addition of the investigated molecule to the aggressive solution, revealing the effectiveness of the molecule as a corrosion inhibitor for copper in 1M HNO_3. A plausible explanation of these

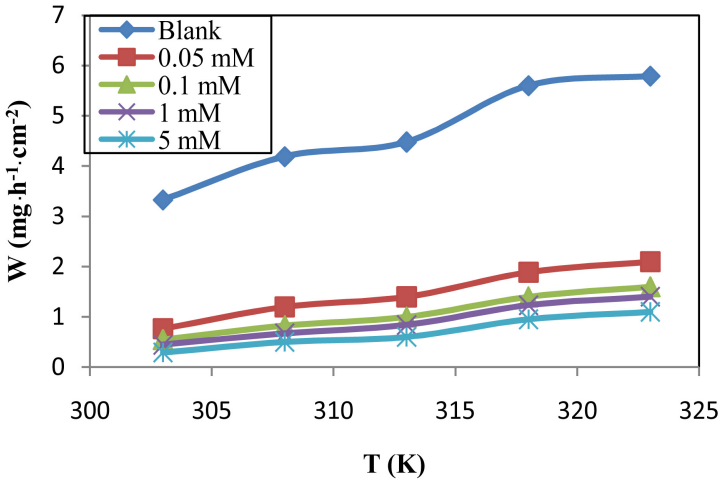

Figure 2. Evolution of corrosion rate with temperature for different concentrations of 7-(2-ethyltiophenyl) theophylline.

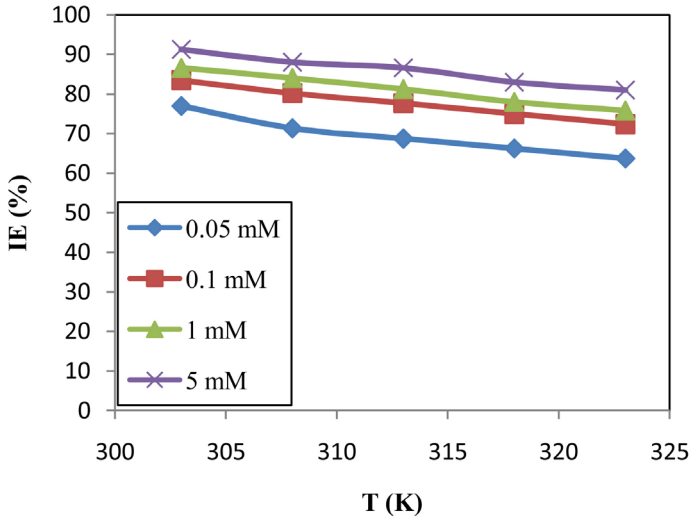

Figure 3. Inhibition efficiency versus temperature for different concentrations of 7-(2-ethyltiophenyl) theophylline.

results is that the increasing inhibitor's concentration reduces the copper exposed surface to the corrosive environment through the increasing number of adsorbed molecules on its surface which hinders the direct acid attack on the metal surface [36]. Furthermore, it has been reported [37] that the decrease in inhibition efficiency with increase in temperature indicates that the process of adsorption of the inhibitor on the corroding metal surface is physical adsorption.

3.2. Adsorption Isotherms

The basic information on the interaction between the inhibitor and the metal can be provided by the adsorption isotherm. The adsorption isotherms tested in this work are the models of Langmuir, Temkin, Freundlich, El-Awady and Flory Huggins. By fitting the degree of surface coverage (θ) and the inhibitor concentration (**Figure 4**), the best adsorption isotherm obtained graphically is Langmuir adsorption isotherm with a strong correlation ($R^2 > 0.999$) and the slopes of the straight lines are close to unity.

The obtained Langmuir adsorption parameters for different temperatures are displayed in **Table 1**.

Given that the correlation coefficients (R^2) and the slopes are very close to unity (**Table 1**), the studied inhibitor adsorbs on copper surface through Langmuir isotherm model.

The values of adsorption equilibrium constant K_{ads} were obtained from the intercepts of the straight lines on the C_{inh}/θ-axis. K_{ads} is related [38] to the standard free adsorption energy ΔG^0_{ads} according to Equation (16):

$$\Delta G^0_{ads} = -RT\ln\left(55.5K_{ads}\right) \tag{16}$$

where 55.5 is the concentration of water in the solution in mol·L^{-1}, R is the perfect gas constant and T is the absolute temperature.

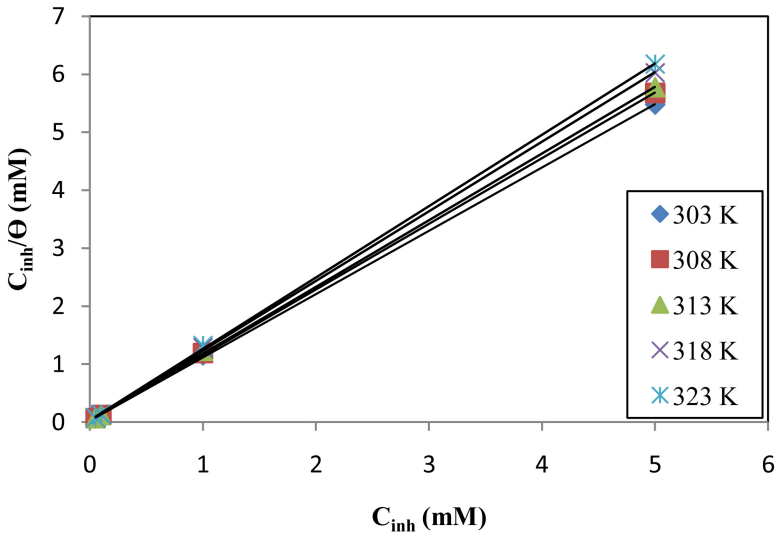

Figure 4. Langmuir adsorption isotherm for 7-(2-ethyltiophenyl) theophylline on copper surface in 1M HNO_3.

Table 1. Regression parameters of Langmuir isotherm.

T(K)	Correlation coefficient	Slope	Intercept
303	0.9999	1.0917	0.0257
308	0.9999	1.1315	0.0259
313	0.9999	1.1496	0.0338
318	0.9999	1.1995	0.0340
323	0.9998	1.2290	0.0374

3.3. Thermodynanmic Adsorption Parameters

The calculated values of ΔG_{ads}^{0} are presented in **Table 2**.

In this work, the calculated values of ΔG_{ads}^{0} for 7-(2-ethyltiophenyl) theophylline were ranging from –36.73 to –38.14 kJ·mol^{-1} which indicated that the adsorption of 7-(2-ethyltiophenyl) theophylline on the copper surface may involve physisorption as well as chemisorption [39] [40] and the decrease in values of K_{ads} with increasing temperature suggested that the desorption process enhances with the increase in temperature [40]. The large negative values of ΔG_{ads}^{0} reveal that the adsorption process takes place spontaneously and the adsorbed layer on the surface of copper is highly stable [41].

The standard adsorption enthalpy change ΔH_{ads}^{0} and the standard adsorption entropy change ΔS_{ads}^{0} are correlated with standard Gibbs free energy by Equation (17):

$$\Delta G_{ads}^{0} = \Delta H_{ads}^{0} - T\Delta S_{ads}^{0} \tag{17}$$

The plot of ΔG_{ads}^{0} versus T (**Figure 5**) leads to the determination of ΔH_{ads}^{0} and ΔS_{ads}^{0} as regression parameters with ΔH_{ads}^{0} as the intercept and ΔS_{ads}^{0} as the negative of the slope of the straight line obtained.

The negative values of ΔH_{ads}^{0} indicate that the adsorption of the inhibitor is

Table 2. Thermodynamic parameters for the adsorption of 7-(2-ethyltiophenyl) theophylline on copper surface at different temperatures.

$T(K)$	K_{ads} (M^{-1})	ΔG^0_{ads} $(kJ \cdot mol^{-1})$	ΔH^0_{ads} $(kJ \cdot mol^{-1})$	ΔS^0_{ads} $(J \cdot mol^{-1} \cdot K^{-1})$
303	38910.51	−36.73		
308	38610.04	−37.31		
313	29858.80	−37.22	−16.62	66.50
318	29411.76	−37.80		
323	26737.97	−38.14		

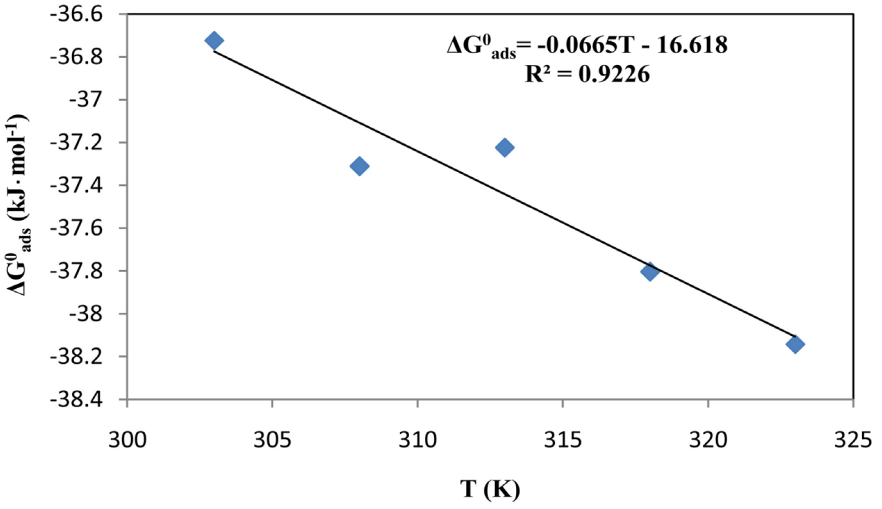

Figure 5. ΔG^0_{ads} versus T for the adsorption of 7-(2-ethyltiophenyl) theophylline on copper in 1M HNO_3.

an exothermic process. Literature [42] pointed out that an exothermic process signifies either physisorption or chemisorption while an endothermic process is associated to chemisorption. Therefore this result confirms that the adsorption process is both consistent with physisorption and chemisorption. The positive values of ΔS^0_{ads} denote a disorder, probably due to desorption of water molecules.

3.4. Effect of Temperature and Thermodynamic Activation Parameters

Temperature is an important parameter in metal dissolution studies [43]. Activation parameters are also of great importance in the study of the inhibition processes. The kinetics functions for the dissolution of copper without and with various concentrations of the tested compound are obtained [44] by applying the Arrhenius equation and the transition state equation:

$$\log W = \log k - \frac{E_a}{2.303RT} \tag{18}$$

$$\log\left(\frac{W}{T}\right) = \left[\log\left(\frac{R}{\aleph h}\right) + \frac{\Delta S^*_a}{2.303R}\right] - \frac{\Delta H^*_a}{2.303RT} \tag{19}$$

In these equations, E_a is the activation energy, k is the Arrhenius pre-exponential factor; h is the Planck's constant, $\aleph$ is the Avogadro number, ΔS_a^* is the change in activation entropy and ΔH_a^* is the change in activation enthalpy.

Figure 6 and Figure 7 show respectively the plots $\log W$ and $\log(W/T)$ versus $1/T$.

All graphs show, both in absence and presence of 7-(2-ethyltiophenyl) theophylline excellent linearity as expected from Equations (18) and (19) respectively. The intercepts of the lines in Figure 6 allow the calculation of the values of the pre-exponential factor (k) and the slopes $\left(-\frac{E_a}{2.303R}\right)$ lead to the determination of the activation energy E_a both in the absence and presence of the inhibitor.

The straight lines obtained by plotting $\log(W/T)$ versus $1/T$ (Figure 7) have a slope of $\left(-\frac{\Delta H_a^*}{2.303R}\right)$ and an intercept of $\left[\log\left(\frac{R}{\aleph h}\right)+\frac{\Delta S_a^*}{2.303R}\right]$. Therefore, the values of ΔH_a^* and ΔS_a^* were calculated and displayed in Table 3.

From Table 3, it seems that E_a and ΔH_a^* varied in the same manner increasing with the concentration, probably due to the thermodynamic relation between them ($\Delta H_a^* = E_a - RT$). The literature [45] states that physical adsorption is associated with, E_a values of the inhibited solution higher than that of the free acid solution (blank). In our work, the uninhibited solution is associated with E_a value, less than that of the inhibited solutions, confirming the predominance of physisorption. Since corrosion primarily occurs at surface sites free of adsorbed inhibitor, the higher E_a values in inhibited solutions imply that the inhibitor mechanically screens the active sites of copper surface thereby decreasing the surface area available for corrosion [46] [47]. The change in activation enthalpy ΔH_a^* has a positive sign, denoting an endothermic activation

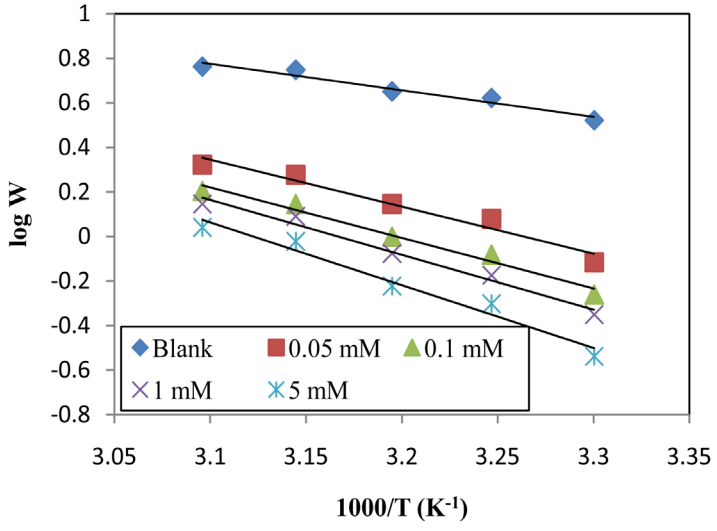

Figure 6. Arrhenius plots for Copper corrosion in 1M HNO_3 solutions without and with 7-(2-ethyltiophenyl) theophylline.

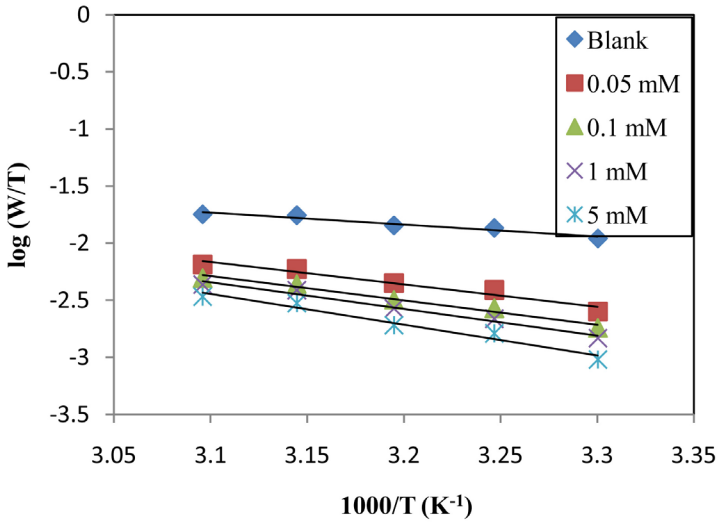

Figure 7. Transition state plots for copper corrosion in 1M HNO_3 with or without 7-(2-ethyltiophenyl) theophylline.

Table 3. Activation parameters for copper corrosion without and with 7-(2-ethyltiophenyl) theophylline in 1M HNO_3.

	E_a (kJ·mol^{-1})	ΔH_a^* (kJ·mol^{-1})	ΔS_a^* (J·mol^{-1}·K^{-1})
Blank	22.77	20.15	−167.87
0.05 mM	40.34	37.69	−121.73
0.1 mM	43.35	40.69	−114.80
1 mM	47.15	44.49	−104.08
5 mM	53.98	51.31	−84.87

process. The shift towards positive value of entropy change (ΔS) implies that the activated complex in the rate determining step represents dissociation rather than association, meaning that disordering increases on going from reactants to the activated complex [48].

3.5. Surface Characterization

Scanning electron micrographs of copper surface before and after immersion in 1M HNO_3 without and with inhibitor are shown in **Figures 8(a)-(c)**.

As presented in **Figure 8(a)**, the metallic sample before immersion in 1M HNO_3 seems smoother and shows fewer pits and cracks. **Figure 8(b)** shows aggressive attack of the corroding medium on the copper surface. The corrosion products appear too uneven, arranged layer upon layer and the metallic surface presents high roughness because of pits and cracks. From **Figure 8(c)**, it is obvious that the copper surface seems to be almost unaffected by corrosion due to the adsorption of 7-(2-ethyltiophenyl) theophylline which was forming a thin inhibitor film of the studied molecule onto copper surface. These results prove that 7-(2-ethyltiophenyl) theophylline protects effectively the metal surface by covering it with a protective layer which separates copper from the corrosive

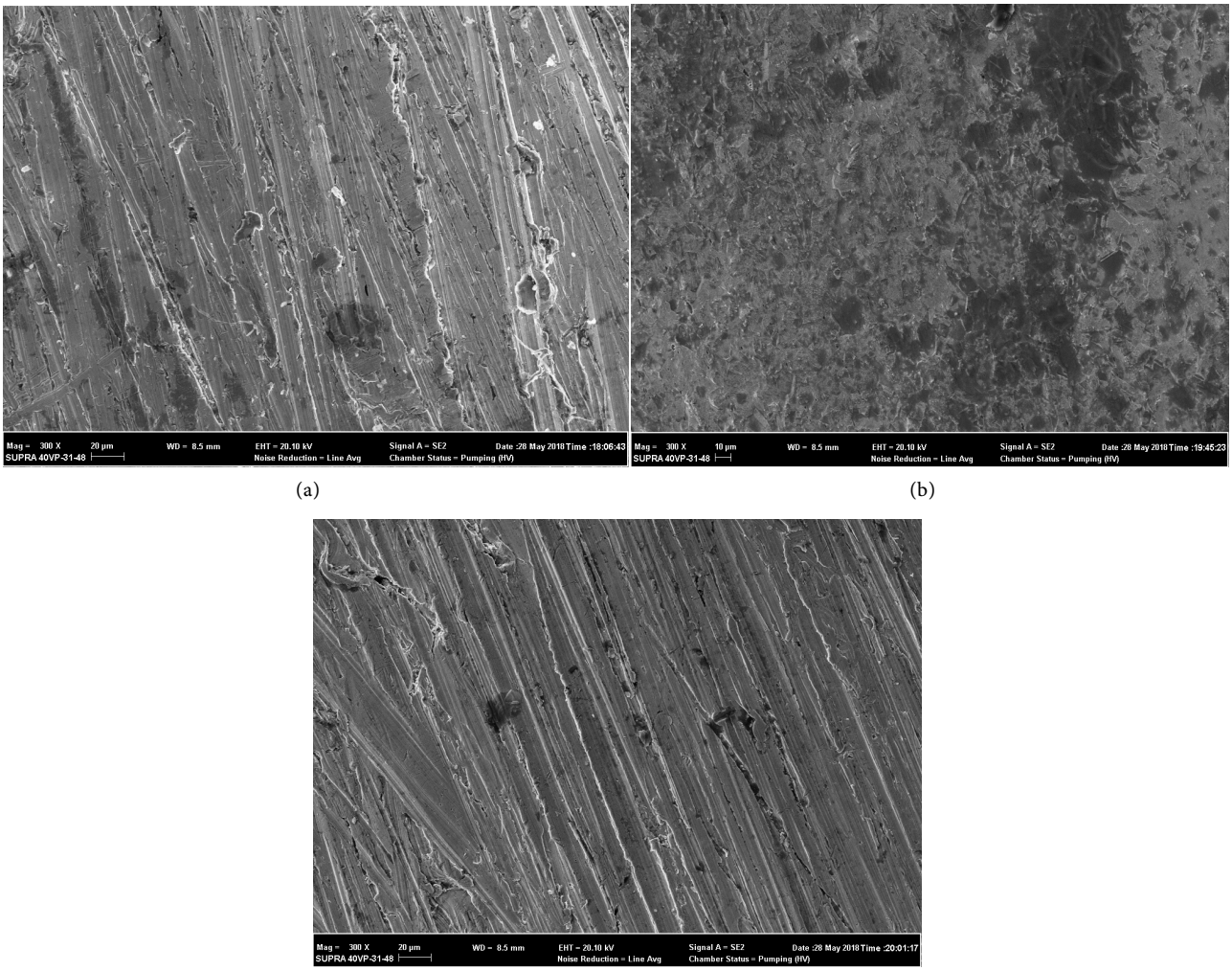

Figure 8. (a) SEM images of polished copper surface: before immersion; (b) after 1h of immersion in 1M HNO_3 solution without inhibitor and (c) after 1 h of immersion in 1M HNO_3 solution with optimal concentration (5 mM) of 7-(2-ethyltiophenyl) theophylline.

environment, confirming the earlier gravimetric results.

3.6. Quantum Chemical Calculations

3.6.1. Global Reactivity

According to the frontier molecular orbital (FMO) theory of chemical reactivity, transition of electron is due to interaction between highest occupied molecular orbital (HOMO) and lowest unoccupied molecular orbital (LUMO) of reacting species. E_{HOMO} [49] measures the tendency towards the donation of electron by a molecule whereas E_{LUMO} indicates the ability of the molecule to accept electrons. The binding ability of the inhibitor to the metal surface [49] increases with increasing of the HOMO and decreasing of the LUMO energy values. The calculated quantum chemical and reactivity parameters are displayed in **Table 4**.

The inhibitor does not only donate electron to the unoccupied d orbital of the metal ion but can also accept electron from the d orbital of the metal, leading to

Table 4. Values of some molecular descriptors.

Descriptor	Value	Descriptor	Value
E_{HOMO} (eV)	−5.8876	I (eV)	5.8876
E_{LUMO} (eV)	−0.8376	A (eV)	0.8376
ΔE (eV)	5.0500	μ (Debye)	5.3036
ΔN	0.3203	η (eV)	2.5250
S (eV)$^{-1}$	0.3960	ω	2.2390
χ (eV)	3.3626	E (a.u)	−1348.9457

the formation of a feedback bond. The highest value of E_{HOMO} −5.8876 eV of 7-(2-ethyltiophenyl) theophylline could explain its good inhibition efficiency (91.29% at $C_{inh} = 5$ mM and $T = 303$ K).

The energy gap ($\Delta E = E_{LUMO} - E_{HOMO}$) is an important parameter as a function of reactivity of the inhibitor molecule towards the adsorption on the metallic surface. As ΔE decreases, the reactivity of the molecule increases leading to increase in the inhibition efficiency of the molecule. Lower values of the energy difference will render good inhibition efficiency, because the energy to remove an electron from the last occupied orbital will be low [50]. In our case, the low value of energy gap (ΔE = 5.0500 eV) could explain the high inhibition efficiency values obtained. HOMO and LUMO diagrams of the inhibitor are given in **Figure 9(a)** and **Figure 9(b)**.

Analyzing **Figure 9**, one can see that HOMO and LUMO densities are concentrated in nearly the same region (around the phenyl ring). So, this region is probably the active area where transfers of electrons could be done (from the molecule to copper or vice-versa).

Ionization energy I and electron affinity A are two important parameters associated with the HOMO and LUMO Energies. The ionization potential (I) and the electronic affinity (A) are respectively (5.8876 eV) and (0.8376 eV). This low value of (I) and the high value of electron affinity indicate the capacity of the molecule both to donate and accept electron.

The dipole moment (μ in Debye) is another important electronic parameter that results from non uniform distribution of charges on the various atoms in the molecule. The high value of dipole moment probably increases the adsorption between chemical compound and metal surface [51]. The energy of the deformability increases with the increase in μ, making the molecule easier to adsorb at the copper surface. The volume of the inhibitor molecules also increases with the increase of μ. This increases the contact area between the molecule and surface of copper and increasing the corrosion inhibition ability of 7-(2-ethyltiophenyl) theophylline. In our work the value 5.3036 (Debye) of the studied inhibitor shows its better inhibition efficiency.

Electronegativity (χ), hardness (η) and softness (S) are very useful parameters in chemical reactivity theory. Electronegativity indicates the capacity of a system to attract electrons, whereas hardness and softness express the degree of reactivity

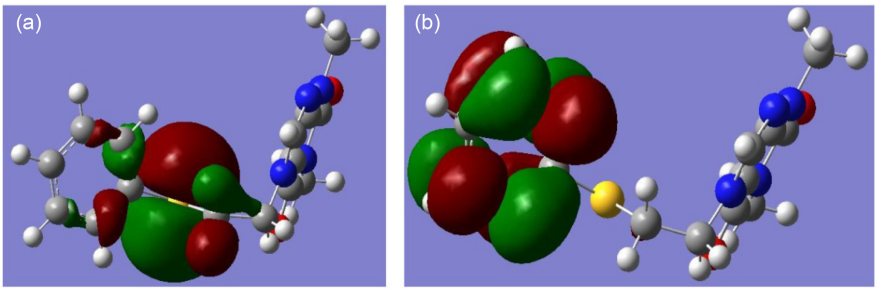

Figure 9. HOMO (a) and LUMO (b) by B3LYP/6-31G (d, p).

of the system. In our study, the electronegativity of the studied molecule ($\chi_{inh} = 3.3626$ eV) is lower than the theoretical value of χ_{Cu} ($\chi_{Cu} = 4.98$ eV) [31], showing that copper has the better attraction capacity. This situation leads to a positive value of electron transferred ($\Delta N = 0.3203$) indicating a possible motion of electrons from the inhibitor to the metal. The electrophilicity index (ω) [31] measures the propensity of chemical species to accept electrons; a high value of electrophilicity index describes a good electrophile while a small value of electrophilicity describes a good nucleophile. In our case the high value ($\omega = 2.2390$ eV) expresses the electrophile character of the studied molecule showing the possible transfer of electrons from the metal to the inhibitor.

3.6.2. Local Reactivity

Local reactivity descriptors including atomic charges, condensed Fukui functions and local softness indices are collected in **Table 5**.

The analysis of **Table 5** indicates that according to the Fukui theory of reactivity, (16 C) is the nucleophilic attacks center (highest value of f_k^+) when (30 C) is the electrophilic attacks center (highest value of f_k^-).

4. Conclusions

From the results and findings of this study, the following conclusions can be drawn:

- The results obtained from gravimetric method indicate that 7-(2-ethyltiophenyl) theophylline is a good inhibitor for copper corrosion in 1M HNO_3;
- The inhibition efficiency of 7-(2-ethyltiophenyl) theophylline is concentration and temperature dependent;
- 7-(2-ethyltiophenyl) theophylline adsorbs on copper according to Langmuir adsorption isotherm;
- Adsorption thermodynamic functions indicate a spontaneous process of physisorption and chemisorption with a predominant physisorption;
- SEM images confirm formation of a protective layer on the copper surface in presence of 7-(2-ethyltiophenyl) theophylline inhibitor;
- There is a good correlation between the quantum chemical (molecular and reactivity) parameters and the experimental data.

Table 5. Atomic charges, condensed Fukui functions and local softness values of 7-(2-ethyltiophenyl) theophylline.

Atom	$q_k(N+1)$	$q_k(N)$	$q_k(N-1)$	f_k^+	f_k^-	s_k^+	s_k^-
1C	0.426	0.475	0.525	−0.049	−0.050	−0.019	−0.020
2C	0.223	0.231	0.261	−0.008	−0.030	−0.003	−0.012
3N	−0.597	−0.508	−0.595	−0.089	0.087	−0.035	0.034
4C	0.770	0.789	0.808	−0.019	−0.019	−0.008	−0.008
5O	−0.583	−0.528	−0.450	−0.055	−0.078	−0.022	−0.031
6N	−0.578	−0.591	−0.594	0.013	0.003	0.005	0.001
7C	−0.151	−0.171	−0.187	0.020	0.016	0.008	0.006
11C	0.552	0.655	0.682	−0.103	−0.027	−0.041	−0.011
12O	−0.609	−0.542	−0.488	−0.067	−0.054	−0.027	−0.021
13N	−0.522	−0.506	−0.537	−0.016	0.031	−0.006	0.012
14C	0.208	0.286	0.323	−0.078	−0.037	−0.031	−0.015
15N	−0.551	−0.525	−0.484	−0.026	−0.041	−0.010	−0.016
16C	**−0.051**	**−0.097**	**−0.086**	**0.046**	**−0.011**	**0.018**	**−0.004**
19C	−0.324	−0.322	−0.401	−0.002	0.079	−0.001	0.031
22S	0.039	0.111	0.293	−0.072	−0.182	−0.029	−0.072
23C	−0.146	−0.136	−0.117	−0.010	−0.019	−0.004	−0.008
24C	−0.094	−0.082	−0.083	−0.012	0.001	−0.005	0.000
25C	−0.093	−0.084	−0.085	−0.009	0.001	−0.004	0.000
26C	−0.080	−0.077	−0.069	−0.003	−0.008	−0.001	−0.003
28C	−0.082	−0.078	−0.069	−0.004	−0.009	−0.002	−0.004
30C	**−0.118**	**0.085**	**−0.069**	**−0.203**	**0.154**	**−0.080**	**0.061**
34C	−0.163	−0.177	−0.196	0.014	0.019	0.006	0.008

Acknowledgements

The authors are grateful to the Laboratory of Physical Chemistry and the Laboratory of Organic Chemistry and Natural Substances of Felix Houphouet-Boigny University, Abidjan, Côte d'Ivoire.

Conflicts of Interest

The authors declare no conflicts of interest regarding the publication of this paper.

References

[1] Zhang, X., He, W., Wallinger, I.O., Pan, J. and Leygraf, C. (2002) Determination of Instantaneous Corrosion Rates and Runoff Rates of Copper from Naturally Patinated Copper during Continuous Rain Events. *Corrosion Science*, **44**, 2131-2151. https://doi.org/10.1016/S0010-938X(02)00015-X

[2] Zhang, X., He, W., Wallinger, I.O. and Leygraf, C. (2014) Mechanistic Studies of Corrosion Product Flaking on Copper and Copper-Based Alloys in Marine Environments. *Corrosion Science*, **85**, 15-25. https://doi.org/10.1016/j.corsci.2014.03.028

[3] Vincent, M., Hartemann, P. and Engels-Deutsch, M. (2016) Antimicrobial Applications of Copper. *International Journal of Hygiene and Environmental Health*, **219**, 585-591. https://doi.org/10.1016/j.ijheh.2016.06.003

[4] Szöcs, E., Vestag, G., Shaban, A., Kouczos, G. and Kalman, E. (1999) Investigation of Copper Corrosion Inhibition by STM and EQCM Techniques. *Journal of Applied Electrochemistry*, **29**, 1339-1345. https://doi.org/10.1023/A:1003869715760

[5] Liu, X. and Astruc, D. (2018) Atomically Precise Copper Nanoclusters and Their Applications. *Coordination Chemistry Reviews*, **359**, 112-126. https://doi.org/10.1016/j.ccr.2018.01.001

[6] Numez, L., Reguera, E., Corvo, F., Gonzalvez, E. and Vasquez, C. (2005) Corrosion of Copper in Seawater and Its Aerosols in a Tropical Island. *Corrosion Science*, **47**, 461-484. https://doi.org/10.1016/j.corsci.2004.05.015

[7] Adeloju, S.B. and Duan, Y.Y. (1994) Influence of Bicarbonate Ions on Stability of Copper Oxides and Copper Pitting Corrosion. *British Corrosion Journal*, **29**, 315-320. https://doi.org/10.1179/000705994798267520

[8] Rocca, E., Bertrand, G., Rapin, C. and Labrune, J.C. (2001) Inhibition of Copper Aqueous Corrosion by Non-Toxic Linear Sodium Heptanoate: Mechanism and ECAFM Study. *Journal of Electroanalytical Chemistry*, **503**, 133-140. https://doi.org/10.1016/S0022-0728(01)00384-9

[9] Vastag, G., Szöcs, E., Shaban, A. and Kalman, E. (2001) New Inhibitors for Copper Corrosion. *Pure and Applied Chemistry*, **73**, 1861-1869. https://doi.org/10.1351/pac200173121861

[10] Trabanelli, G. (1991) Whitney Award Lecture: Inhibitors—An Old Remedy for a New Challenge. *Corrosion*, **47**, 410-419. https://doi.org/10.5006/1.3585271

[11] Antonijevic, M.M. and Petrovic, M.B. (2008) Copper Corrosion Inhibitors. A Review. *International Journal of Electrochemical Science*, **3**, 1-28.

[12] Kouakou, V., Niamien, P.M., Yapo, A.J. and Trokourey, A. (2016) Copper Corrosion Inhibition in 1 M Nitric Acid: Adsorption and Inhibitive Action of Theophylline. *Chemical Science Review and Letters*, **5**, 131-146.

[13] Otmacicm H. and Stupnisek-Lisac, E. (2002) Copper Corrosion Inhibitors in Near Neutral Media. *Electrochimica Acta*, **48**, 985-991. https://doi.org/10.1016/S0013-4686(02)00811-3

[14] Scendo, M., Poddebniak, D. and Malyszko, J. (2003) Indole and 5-Chloroindole as Inhibitors of Anodic Dissolution and Cathodic Deposition of Copper in Acidic Chloride Solutions. *Journal of Applied Electrochemistry*, **33**, 287-293. https://doi.org/10.1023/A:1024117230591

[15] Rodriguez-Valdez, L.M., Martinez-Villafane, A. and Glossman-Mitnik, D. (2005) CHIH-DFT Theoretical Study of Isomeric Thiatriazoles and Their Potential Activity as Corrosion Inhibitors. *Journal of Molecular Structure*: *THEOCHEM*, **716**, 61-65.

[16] Stoyanova, A.E. and Peyerimhoff, S.D. (2002) On the Relationship between Corrosion Inhibiting Effect and Molecular Structure. *Electrochimica Acta*, **47**, 1365-1371. https://doi.org/10.1016/S0013-4686(01)00874-X

[17] Finsgar, M., Lesar, A., Kokaij, A. and Milosev, I. (2008) A Comparative Electrochemical and Quantum Chemical Calculation Study of BTAH and BTAOH as Copper Corrosion Inhibitors in Near Neutral Chloride Solution. *Electrochimica Acta*, **53**, 8287-8297. https://doi.org/10.1016/j.electacta.2008.06.061

[18] Sanderson, R.T. (1952) An Interpretation of Bond Lengths in Alkali Halide Gas Molecules. *Journal of the American Chemical Society*, **74**, 272-274. https://doi.org/10.1021/ja01121a522

[19] Hohenberg, P. and Kohn, W. (1964) Inhomogeneous Electron Gas. *Physical Review Journals Archive*, **136**, B864-B871. https://doi.org/10.1103/PhysRev.136.B864

[20] Parr, R.G. and Yang, W. (1984) Density Functional Approach to Frontier-Electron Theory of Chemical Reactivity. *Journal of the American Chemical Society*, **106**, 4049-4050. https://doi.org/10.1021/ja00326a036

[21] Wang, H., Wang, X., Wang, H., Wang, L. and Liu, A. (2007) DFT Study of New Bipyrazole Derivatives and Their Potential Activity as Corrosion Inhibitors. *Journal of Molecular Modeling*, **13**, 147-153. https://doi.org/10.1007/s00894-006-0135-x

[22] Fang, J. and Li, J. (2002) Quantum Chemistry Study on the Relationship between Molecular Structure and Corrosion Inhibition Efficiency of Amides. *Journal of Molecular Structure*: *THEOCHEM*, **593**, 179-185.

[23] Arslan, T., Kandamirli, F., Ebenso, E.E., Love, I. and Alemu. H. (2009) Quantum Chemical Studies on the Corrosion Inhibition of Some Sulphonamides on Mild Steel in Acidic Medium. *Corrosion Science*, **51**, 35-47. https://doi.org/10.1016/j.corsci.2008.10.016

[24] Frisch, M.J., Trucks, G.W., Schlegel, G.E.S.H.B., Robb, M.A., Cheeseman, J.R., Scalmani, G., Barone, V., Mennucci, B., Petersson, G.A., Nakatsuji, H., Caricato, M., Li, X., Hratchian, H.P., Izmaylov, A.F., Bloino, J., Zheng, G., Sonnenberg, J.L., Hada, M., Ehara, M., Toyota, K., Fukuda, R., Hasegawa, J., Ishida, M., Nakajima, T., Honda, Y., Kitao, O., Nakai, H., Vreven, T., Montgomery Jr., J.A., Peralta, J.E., Ogliaro, F., Bearpark, M., Heyd, J.J., Brothers, E., Kudin, V.N.S.K.N., Kobayashi, R., Normand, J., Raghavachari, K., Rendell, A., Burant, J.C., Iyengar, S.S., Tomasi, J., Cossi, M., Rega, N., Millam, J.M., Klene, M., Knox, J.E., Cross, J.B., Bakken, V., Adamo, R., Jaramillo, C., Gomperts, J., Stratmann, R., Yazyev, R.E., Austin, O., Cammi, A.J., Pomelli, C., Ochterski, J.W., Martin, R.L., Morokuma, K., Zakrzewski, V.G., Voth, G.A., Salvador, P., Dannenberg, J.J., Dapprich, S., Daniels, A.D., Farkas, O., Foresman, J.B., Ortiz, J.V., Cioslowski, J. and Fox, D.J. (2009) Gaussian 09, Revision A.02. Gaussian, Inc., Wallingford, CT.

[25] Becke, A.D. (1993) Density Functional Thermochemistry. III. The Role of Exact Exchange. *The Journal of Chemical Physics*, **98**, 5648-5652. https://doi.org/10.1063/1.464913

[26] Lee, C., Yang, W. and Parr, R.G. (1988) Development of the Colle Salvetti Correlation-Energy Formula into a Functional of the Electron Density. *Physical Review B*, **37**, 785-789. https://doi.org/10.1103/PhysRevB.37.785

[27] Miehlich, B., Savin, A., Stoll, H. and Preuss, H. (1989) Results Obtained with the Correlation Energy Density Functionals of Becke and Lee, Yang and Parr. *Chemical Physics Letters*, **157**, 200-206. https://doi.org/10.1016/0009-2614(89)87234-3

[28] Zhang, S.G., Lei, W., Xia, M.Z. and Wang, F.Y. (2005) QSAR Study on N-Containing Corrosion Inhibitors: Quantum Chemical Approach Assisted by Topological Index. *Journal of Molecular Structure*: *THEOCHEM*, **732**, 173-182. https://doi.org/10.1016/j.theochem.2005.02.091

[29] Koopmans, T. (1934) Über die Zuordnung von Wellenfunktionen und Eigenwerten zu den Einzelnen Elektronen Eines Atoms. *Physica*, **1**, 104-113. https://doi.org/10.1016/S0031-8914(34)90011-2

[30] Pearson, R.G. (1988) Absolute Electronegativity and Hardness: Application to Inorganic Chemistry. *Inorganic Chemistry*, **27**, 734-740. https://doi.org/10.1021/ic00277a030

[31] Parr, R.G., Szentpaly, L.V. and Liu, S. (1999) Electrophilicity Index. *Journal of the American Chemical Society*, **121**, 1922-1924. https://doi.org/10.1021/ja983494x

[32] Ebenso, E.E., Arslan, T., Kandemirli, F., Caner, I.N. and Love, I.I. (2010) Quantum Chemical Studies of Some Rhodamine Azosulpha Drugs as Corrosion Inhibitors for Mild Steel in Acidic Medium. *International Journal of Quantum Chemistry*, **110**, 1003-1018. https://doi.org/10.1002/qua.22249

[33] Fuentealba, P., Perez, P. and Contreras, R. (2000) On the Condensed Fukui Function. *The Journal of Chemical Physics*, **113**, 2544-2551. https://doi.org/10.1063/1.1305879

[34] Quijano, M.A., Palomar-Pardavé, M., Cuan, A., Romo, M.R., Silva, G.N., Bustamante, R.A., *et al*. (2011) Quantum Chemical Study of 2-Mercaptoimidazole, 2-Mercaptobenzimidazole, 2-Mercapto-5-Methylbenzimidazole and 2-Mercapto-5-Nitrobenzimidazole as Corrosion Inhibitors for Steel. *International Journal of Electrochemical Science*, **6**, 3729-3742.

[35] Yang, W. and Mortier, W.J. (1986) The Use of Global and Local Molecular Parameters for the Analysis of the Gas-Phase Basicity of Amines. *Journal of the American Chemical Society*, **108**, 5708-5711. https://doi.org/10.1021/ja00279a008

[36] Diki, N.Y.S., Bohoussou, K.V., Kone, M.G.-R., Ouedraogo, A. and Trokourey, A. (2018) Cefadroxil Drug as Corrosion Inhibitor for Aluminum in 1 M HCl Medium: Experimental and Theoretical Studies. *IOSR Journal of Applied Chemistry*, **11**, 24-36.

[37] Saratha, R. and Meenakshi, R. (2010) Corrosion Inhibitor: A Plant Extract. *Der Pharma Chemica*, **2**, 287-294.

[38] Khamis, E. (1990) The Effect of Temperature on the Acidic Dissolution of Steel in the Presence of Inhibitors. *Corrosion*, **46**, 476-484. https://doi.org/10.5006/1.3585135

[39] Khaled, K.F. and Hackerman, N. (2004) Ortho-Substituted Anilines to Inhibit Copper Corrosion in Aerated 0.5 M Hydrochloric Acid. *Electrochimica Acta*, **49**, 485-495. https://doi.org/10.1016/j.electacta.2003.09.005

[40] Quraishi, M.A., Singh, A., Singh, V.K., Yadav, D.K. and Singh, A.K. (2010) Green Approach to Corrosion Inhibition of Mild Steel in Hydrochloric Acid and Sulphuric Acid Solutions by the Extract of Murraya Koenigii Leaves. *Materials Chemistry and Physics*, **22**, 114-122. https://doi.org/10.1016/j.matchemphys.2010.02.066

[41] Scendo, M. and Hepel, M. (2008) Inhibiting Properties of Benzimidazole Films for Cu(II)/Cu(I) Reduction in Chloride Media Studied by RDE and EQCN Techniques. *Journal of Electroanalytical Chemistry*, **613**, 35-50. https://doi.org/10.1016/j.jelechem.2007.10.014

[42] Durnie, W., Marco, R.D., Jefferson, A. and Kinsella, B. (1999) Development of a Structure-Activity Relationship for Oil Field Corrosion Inhibitors. *Journal of The Electrochemical Society*, **146**, 1751-1756. https://doi.org/10.1149/1.1391837

[43] Souza, F.S.D. and Spinelli, A. (2009) Caffeic Acid as a Green Corrosion Inhibitor for Mild Steel. *Corrosion Science*, **51**, 642-649. https://doi.org/10.1016/j.corsci.2008.12.013

[44] Li, X., Deng, S., Fu, H. and Mu, G. (2008) Synergistic Inhibition Effect of Rare Earth Cerium (IV) Ion and Anionic Surfactant on the Corrosion of Cold Rolled Steel in H_2SO_4 Solution. *Corrosion Science*, **50**, 2635-2645. https://doi.org/10.1016/j.corsci.2008.06.026

[45] Martinez, S. and Stern, I. (2001) Inhibitory Mechanism of Low-Carbon steel Corrosion by Mimosa Tannin in Sulphuric Acid Solutions. *Journal of Applied Electrochemistry*, **31**, 973-978. https://doi.org/10.1023/A:1017989510605

[46] Alinnor, I.J. and Ejikeme, P.M. (2012) Corrosion Inhibition of Aluminium in Acidic

Medium by Different Extracts of Ocimum Gratissimum. *American Chemical Science Journal*, **2**, 122-135. https://doi.org/10.9734/ACSJ/2012/1835

[47] Diki, N.Y.S., Gbassi, G.K., Ouedraogo, A., Berte, M. and Trokourey, A. (2018) Aluminum Corrosion Inhibition by Cefixime Drug: Experimental and DFT Studies. *Journal of Electrochemical Science and Engineering*, **8**, 302-320.

[48] Ansari, K.R., Yadav, D.K., Ebenso, E.E. and Quraishi, M.A. (2012) Novel and Effective Pyridyl Substituted 1,2,4-Triazole as Corrosion Inhibitor for Mild Steel in Acid Solution. *International Journal of Electrochemical Science*, **7**, 4780-4799.

[49] Gece, G. and Bilgic, S. (2009) Quantum Chemical Study of Some Cyclic Nitrogen Compounds as Corrosion Inhibitors of Steel in NaCl Media. *Corrosion Science*, **51**, 1876-1878. https://doi.org/10.1016/j.corsci.2009.04.003

[50] Obot, I.B., Obi-Egbedi, N.O. and Umoren, S.A. (2009) Adsorption Characteristics and Corrosion Inhibitive Properties of Clotrimazole for Aluminium Corrosion in Hydrochloric Acid. *International Journal of Electrochemical Science*, **4**, 863-877.

[51] Li, X., Deng, S., Fu, H. and Li, T. (2009) Adsorption and Inhibition Effect of 6-Benzylaminopurine on Cold Rolled Steel in 1.0 M HCl. *Electrochimica Acta*, **54**, 4089-4098. https://doi.org/10.1016/j.electacta.2009.02.084